Plasmenylcholine and Phosphatidylcholine Membrane Bilayers Possess Distinct Conformational Motifs†

Xianlin Han and Richard W. Gross*
Molecular and Cellular Cardiovascular Biochemistry, Washington University School of Medicine, St. Louis, Missouri 63110
Received November 9, 1989; Revised Manuscript Received February 22, 1990

ABSTRACT: The conformation of plasmenylcholine near the hydrophobic–hydrophilic interface in membrane bilayers was deduced by determination of critical internuclear distances utilizing truncated driven nuclear Overhauser enhancement. These experiments demonstrated that the β-vinyl ether proton in plasmenylcholine was in close spatial proximity and nearly equidistant (~3 Å) to both the α- and β-methylene protons of the *sn*-2 aliphatic chain. In contrast, the distances between the α-vinyl ether proton and the α- and β-methylene protons of the *sn*-2 aliphatic chain were ≥5 Å. Furthermore, the distance between the N–CH_3 protons in the polar head group and the methylene protons of the glycerol backbone in plasmenylcholine vesicles is larger than that present in phosphatidylcholine vesicles. Although the proximal portion of the *sn*-2 acyl chain in phosphatidylcholine is bent, conformational analysis utilizing these distance constraints demonstrated that the carbon atoms which comprise the proximal portion of the *sn*-2 aliphatic chain in plasmenylcholine are nearly coplanar, in register, and parallel to the *sn*-1 aliphatic chain. Taken together, these observations indicate that modest covalent alterations in the proximal portion of the *sn*-1 aliphatic chain in choline glycerophospholipids result in substantial changes in the molecular conformation and packing of hydrated phospholipid bilayers.

Although the existence of plasmalogens has been known for over 60 years (Feulgen & Voit, 1924), the reasons underlying their predominance in specific biologic membranes have remained elusive. For example, plasmalogen molecular species are the predominant phospholipid constituents present in the electrically active membrane of cardiac myocytes (i.e., sarcolemma) (Gross, 1984), but their role in facilitating ion channel or ion pump function is unknown. Furthermore, analyses of plasmalogen molecular species reveal that they are highly enriched in arachidonic acid and that they represent the major phospholipid storage depot for arachidonic acid in several cell types (Mueller et al., 1983; Gross, 1984, 1985; Ford & Gross, 1989a). The identification of a plasmalogen-selective phospholipase A_2 which is activated by physiologic increments in calcium ion concentration (Loeb & Gross, 1986), in conjunction with the demonstration that plasmalogens are rapidly hydrolyzed during cellular stimulation (Chilton & Murphy, 1986; Ford & Gross, 1989b), has further substantiated the importance of plasmalogen molecular species in mediating several types of biologic phenomena. Despite the potential importance of plasmalogens in membrane structure and function, the differences between the molecular conformations of plasmalogens and conventional diacyl phospholipids are unknown.

The stereochemical relationships present in phosphatidylcholine crystals have been determined by X-ray diffraction (Pearson & Pascher, 1979). Remarkably, the proximal portion of the *sn*-2 acyl chain in phosphatidylcholine contains a "bend" that increases the molecular cross-sectional area near the hydrophobic–hydrophilic interface. This bend is uniformly present in hydrated dispersions of phosphatidylcholine as ascertained by ^2H NMR[1] spectroscopy (Seelig & Browning, 1978) and has therefore become a hallmark of biologic membrane structure. Since plasmalogens contain covalent alterations in the proximal portion of the *sn*-1 aliphatic chain, it seems likely that their molecular geometry near the *sn*-2 carboxyl group is altered, thus modifying the structure of the lipid–aqueous interface and potentially influencing their interactions with cellular proteins (e.g., phospholipases, ion channels, ion pumps, receptors, etc.).

In this work, we exploit the substantial differences in the NMR chemical shifts of protons present in the proximal portions of the *sn*-1 and *sn*-2 aliphatic chains in plasmenylcholine to compare the conformation of plasmenylcholine in membrane bilayers with the traditionally accepted conformation of phosphatidylcholine. Determinations of critical internuclear distances utilizing truncated driven nuclear Overhauser enhancement (TDNOE) demonstrated that the proximal portions of the *sn*-1 and *sn*-2 aliphatic chains in plasmenylcholine are in close spatial proximity (~3 Å), in register, and nearly parallel, which contrasts dramatically with the conformation of phosphatidylcholine deduced by X-ray crystallography and ^2H NMR spectroscopy (Pearson & Pascher, 1979; Seelig & Browning, 1978).

Materials and Methods

Materials. Palmitic anhydride, oleic anhydride, and arachidonic anhydride were purchased from Nu Check Prep, Inc. (Elysian, MN). 1-Hexadecanoyl-2-eicosa-5,8,11,14-tetraenoyl-*sn*-glycero-3-phosphocholine (PA phosphatidylcholine) and perdeuterated dipalmitoylphosphatidylcholine (d_{62} PP phosphatidylcholine) were purchased from Avanti Polar

† This research was supported by NIH Grant HL 34839. R.W.G. is the recipient of an Established Investigator award from the American Heart Association.

* Author to whom correspondence should be addressed at Molecular and Cellular Cardiovascular Biochemistry, Washington University School of Medicine, 660 South Euclid Ave., Box 8020, St. Louis, MO 63110.

[1] Abbreviations: NMR, nuclear magnetic resonance; NOE, nuclear Overhauser enhancement; TDNOE, truncated driven NOE; PA plasmenylcholine, 1-*O*-(*Z*)-hexadec-1-enyl-2-eicosa-5,8,11,14-tetraenoyl-*sn*-glycero-3-phosphocholine; PO plasmenylcholine, 1-*O*-(*Z*)-hexadec-1-enyl-2-octadec-9-enoyl-*sn*-glycero-3-phosphocholine; PP plasmenylcholine, 1-*O*-(*Z*)-hexadec-1-enyl-2-hexadecanoyl-*sn*-glycero-3-phosphocholine; PA phosphatidylcholine, 1-hexadecanoyl-2-eicosa-5,8,11,14-tetraenoyl-*sn*-glycero-3-phosphocholine; d_{62} PP phosphatidylcholine, perdeuterated dipalmitoylphosphatidylcholine.

0006-2960/90/0429-4992$02.50/0

Lipids, Inc. (Birmingham, AL). 4-(*N*,*N*-Dimethylamino)-pyridine was obtained from Aldrich Chemical Co. (Milwaukee, WI). Homogeneous 1-*O*-(*Z*)-hexadec-1-enyl-*sn*-glycero-3-phosphocholine (palmitoyllysoplasmenylcholine) was prepared from bovine heart lecithin as previously described (Wolf & Gross, 1985a). 1-*O*-(*Z*)-Hexadec-1-enyl-2-eicosa-5,8,11,14-tetraenoyl-*sn*-glycero-3-phosphocholine (PA plasmenylcholine), 1-*O*-(*Z*)-hexadec-1-enyl-2-octadec-9-enoyl-*sn*-glycero-3-phosphocholine (PO plasmenylcholine), and 1-*O*-(*Z*)-hexadec-1-enyl-2-hexadecanoyl-*sn*-glycero-3-phosphocholine (PP plasmenylcholine) were synthesized by 4-(*N*,*N*-dimethylamino)pyridine-catalyzed condensation of the corresponding anhydride with palmitoyllysoplasmenylcholine as previously described (Wolf & Gross, 1985a).

Preparation of Phospholipid Vesicles. Appropriate amounts of homogeneous phospholipids (30 mM final concentration for single-component phospholipid vesicles or 60 mM final lipid concentration for binary mixtures of plasmenylcholine and perdeuterated phosphatidylcholine) were initially dried with N_2 prior to exhaustive evacuation (50 mTorr) for at least 4 h. Subsequent addition of buffer (0.1 M phosphate/D_2O buffer, pD 7.0) and sonication [12 30-s bursts from a Vibra Cell Model VC600 sonicator (Sonics Materials, Inc., Danbury, CT)] above the phase transition temperature in a N_2 atmosphere resulted in the formation of phospholipid vesicles. The sonicate was centrifugated at $30000g_{max}$ for 20 min to remove small amounts of particulate matter.

NMR Spectroscopy. NMR spectra of phospholipid vesicles were obtained on a Varian XL-300 spectrometer operating at 300 MHz. The sample temperature during experiments was 50 ± 1 °C for PP plasmenylcholine and for PA plasmenylcholine in a d_{62} PP phosphatidylcholine matrix in a 1:5 molar ratio. All other experiments were performed at 25 ± 1 °C. Spectra were collected with 25-μs pulses of 90° duration separated by a delay of 6.5 s, which was greater than 5 times the T_1 of all protons (Han and Gross, unpublished results). Peak assignments were made from homonuclear two-dimensional correlation spectrometry in conjunction with the anticipated chemical shifts of each functional group in plasmenylcholine (Han and Gross, unpublished results). TDNOE experiments were performed as described by Wagner and Wüthrich (1979) with 1000 scans for each difference spectrum. Distances were determined by varying the preirradiation time from 0.02 to 5 s, a saturating field strength of 14.5 Hz being employed. The approximate distance (r) between protons can be obtained from the initial buildup rate (σ) of the observed NOE by the following formalism (Clore & Gronenborn, 1985):

$$r_{ij}/r_{kl} = (\sigma_{kl}/\sigma_{ij})^{1/6} \quad (1)$$

In this work, we utilized the known distance between the α- and β-vinyl ether protons in the *sn*-1 aliphatic chain (2.3 Å) as an internal reference to estimate internuclear distances.

Results and Discussion

Although NOE has been widely employed to provide information on internuclear distances in relatively small molecules [e.g., Noggle and Schirmer (1971)], the strong zero quantum exchange processes stimulated by slow molecular motions in membrane vesicles result in the loss of spatial information with traditional steady-state NOE techniques (Ellena et al., 1985). However, utilization of TDNOE allows quantification of internuclear distances from the kinetics of the buildup of resonance intensity in membrane vesicles since effects from spin diffusion are minimized (Kuroda & Kitamura, 1984). Utilization of TDNOE to assess the geometry of plasmenylcholine vesicles was facilitated by the fact that

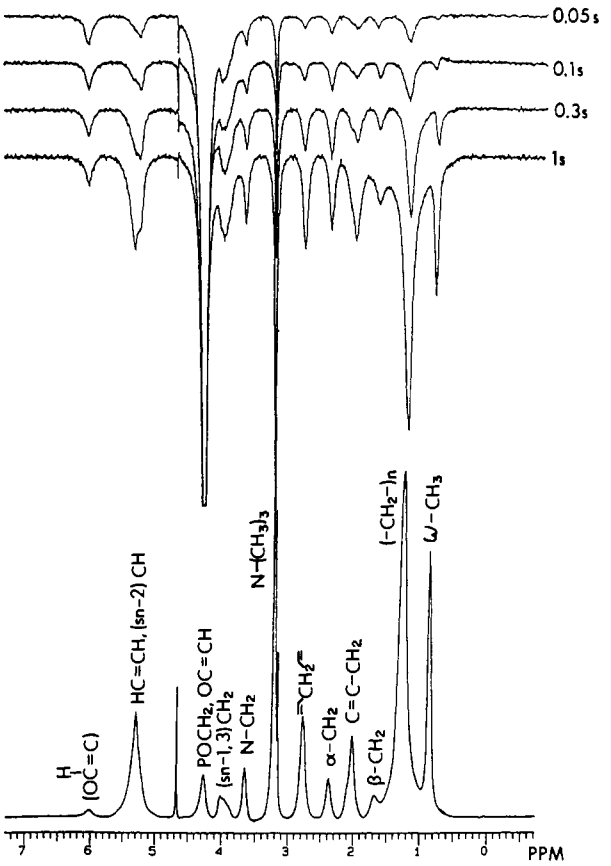

FIGURE 1: (Bottom) Conventional 300-MHz ^1H NMR spectrum of 1-*O*-(*Z*)-hexadec-1-enyl-2-eicosa-5,8,11,14-tetraenoyl-*sn*-glycero-3-phosphocholine (PA plasmenylcholine) vesicles. PA plasmenylcholine (23 mg) was suspended in $CHCl_3$, dried with N_2, and exhaustively evacuated prior to sonication (22 °C) in 0.1 M phosphate/D_2O buffer, pD 7.0 (1 mL). NMR spectra of the PA plasmenylcholine vesicles (30 mM) in the supernatant were obtained with a Varian XL-300 spectrometer operating at 300 MHz, employing 25 μs of 90° pulses separated by a delay of 6.5 s (≥5 times the T_1 of all protons). Peak assignments were made from homonuclear two-dimensional correlation spectroscopy in conjunction with the anticipated chemical shifts of each functional group in plasmenylcholine. All chemical shifts are reported with the internal solvent peak (HOD) as reference with respect to tetramethylsilane as external standard. (Top) Time-dependent nuclear Overhauser enhanced difference spectra of PA plasmenylcholine vesicles. TDNOE experiments were performed on plasmenylcholine vesicles by irradiation of the sonicate at 4.3 ppm (corresponding to the β-vinyl ether proton) with a power level of $\gamma H_2/2\pi \sim 14.5$ Hz. Each difference spectrum was obtained from 1000 scans.

plasmenylcholine contains separate and distinct covalent entities at the *sn*-1 and *sn*-2 positions whose different chemical shifts allow the complete resolution of each proton resonance in the proximal portions of the *sn*-1 and *sn*-2 aliphatic chains (Figure 1, bottom). Thus, assessment of internuclear distances between the proximal portions of each aliphatic chain is possible in plasmenylcholine but is not possible with this technique with either phosphatidylcholine or alkyl ether choline glycerophospholipids.

TDNOE difference spectra of vesicles comprised of PA plasmenylcholine demonstrated resonances that were enhanced by irradiation of the β-vinyl ether proton (Figure 1, top). The kinetics of the increase in integrated resonance intensity after irradiation at 4.3 ppm (β-vinyl ether proton) was substantially different for resonances corresponding to individual protons (Figure 2). As expected, the α-vinyl ether proton most rapidly approached its steady-state resonance enhancement during β-vinyl ether proton irradiation. Remarkably, substantial and exponential increases in the rates of resonance intensity buildup

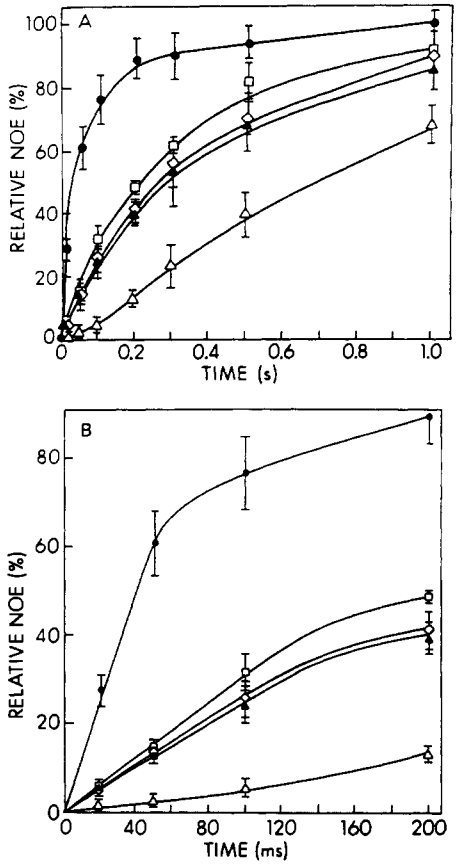

FIGURE 2: Kinetics of TDNOE in PA plasmenylcholine vesicles. (A) PA plasmenylcholine vesicles (30 mM) were prepared and subjected to TDNOE analysis by determination of the rate of buildup of the integrated resonance area as a function of mixing time (20 ms to 5 s) after initiation of irradiation at 4.3 ppm. (B) The initial data during the first 200 ms from panel A have been expanded to facilitate assessment of the initial rate of TDNOE buildup in PA plasmenylcholine vesicles during irradiation at 4.3 ppm. Relative NOE refers to the fraction of the observed NOE to the total NOE at steady state times 100. (●) α-Vinyl ether proton (□) α-methylene protons on the *sn*-2 acyl chain; (◇) β-methylene protons on the *sn*-2 acyl chain; (▲) protons allylic to the vinyl ether linkage; (△) aliphatic terminal methyl protons. All data points represent the $\bar{X} \pm$ SE of at least three entirely independent preparations.

in both the α- and β-methylene protons of the *sn*-2 aliphatic chain were also present during irradiation at 4.3 ppm. By use of the known distance between each vinyl proton in the vinyl ether linkage (2.3 Å) as an internal reference, the distances between the α- and β-methylene protons and the β-vinyl ether proton were deduced by internal comparisons of their respective first-order rate constants for TDNOE buildup (eq 1). The results indicate that both the α- and β-methylene protons were ~3 Å from the β-vinyl ether proton. Although the temporal buildup of resonance intensity was clearly exponential for the α- and β-methylene protons, the increase in NOE for the aliphatic terminal methyl protons was sigmoidal, demonstrating that the observed augmentation of resonance intensity for the aliphatic terminal methyl protons was due to spin diffusion.

To identify the distance between the α- and β-methylene protons and the α-vinyl ether proton, additional experiments were performed. Irradiation of hydrated plasmenylcholine vesicles at 6.0 ppm (α-vinyl ether proton) resulted in the rapid buildup of resonance intensity at 4.3 ppm (β-vinyl ether proton), demonstrating the anticipated dipolar coupling between the α- and β-vinyl ether protons. However, no significant buildup in the resonance intensities of either the α- or β-methylene protons of the *sn*-2 aliphatic chain or the protons

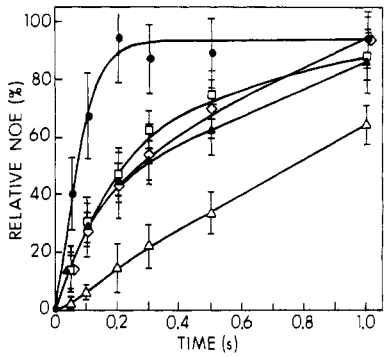

FIGURE 3: Kinetics of TDNOE in vesicles comprised of equimolar plasmenylcholine/phosphatidylcholine. Equimolar mixtures of PA plasmenylcholine and perdeuterated dipalmitoylphosphatidylcholine [30 mM of each lipid (60 mM total lipid concentration)] were dissolved in $CHCl_3$, evaporated with nitrogen, and evacuated at low pressure for 2 h. 1 mL of 0.1 M phosphate/D_2O buffer, pD 7, was added to the lipid mixture, which was subsequently sonicated, and TDNOE difference spectra were acquired during irradiation at 4.3 ppm. Relative NOE refers to the fraction of the observed NOE to the total NOE at steady state times 100. (●) α-Vinyl ether proton (□) α-methylene protons on the *sn*-2 acyl chain; (◇) β-methylene protons on the *sn*-2 acyl chain; (▲) protons allylic to the vinyl ether linkage; (△) aliphatic terminal methyl protons. All data points represent the $\bar{X} \pm$ SE of at least three entirely independent preparations.

allylic to the β-vinyl ether carbon was present at early irradiation times during irradiation at 6.0 ppm. These results indicate that the α-vinyl ether proton is at least 5 Å away from either the α- or β-methylene protons of the *sn*-2 acyl chain.

Similarly, parallel experiments utilizing PO plasmenylcholine and PP plasmenylcholine demonstrated a rapid buildup of resonance intensity between the α- and β-methylene protons of the *sn*-2 aliphatic chain during irradiation of the β-vinyl ether proton. No resonance enhancement of the α- or β-methylene protons was detected at early time points during irradiation at 6.0 ppm. Accordingly, the close spatial proximity of the aliphatic constituents in the proximal portions of the *sn*-1 and *sn*-2 positions likely reflects the subclass-specific conformation of plasmenylcholine vesicles and is largely independent of the type of fatty acid present at the *sn*-2 position in plasmenylcholine (i.e., individual molecular species).

Since ^1H–^1H NOE is mediated by through-space dipolar interactions, these results do not distinguish between inter- and intramolecular nuclear spin exchange in vesicles where lipid aggregates possess high molecular densities. To discriminate between these possibilities, vesicles comprised of equimolar mixtures of plasmenylcholine and perdeuterated phosphatidylcholine were prepared. Dilution of nearest-neighbor interactions by addition of equimolar perdeuterated dipalmitoylphosphatidylcholine did not attenuate the absolute intensity of the observed NOE, its kinetic rate of buildup, or its relative rate of buildup in PA plasmenylcholine (Figure 3). Furthermore, experiments utilizing 1:5 molar ratios of PA plasmenylcholine/d_{62} PP phosphatidylcholine did not demonstrate any attenuation of the kinetics of NOE buildup at either 50 or 100 ms (i.e., ~20 and ~40% of the saturating NOE in the α- and β-methylene protons was present at 50 and 100 ms during β-vinyl ether proton irradiation). If lateral diffusion in plasmenylcholine vesicles is similar to that in phosphatidylcholine, then it is likely that each molecule of plasmenylcholine interacts with many perdeuterated phosphatidylcholine molecules even at the earliest time point measured. Since there were no measurable differences in the observed kinetics of resonance enhancement (in direct comparisons to the vinyl ether ^1H–^1H enhancement which is known to be intramolecular) in the presence or absence of per-

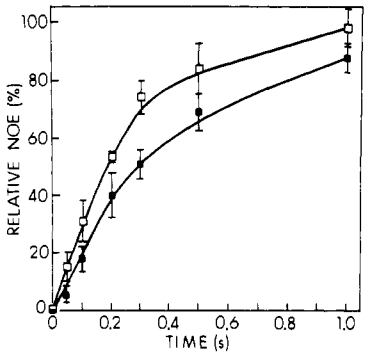

FIGURE 4: Temporal dependence of NOE buildup of the glycerol methylene protons during irradiation of the choline methyl protons in PA plasmenylcholine vesicles and PA phosphatidylcholine vesicles. PA plasmenylcholine vesicles [30 mM (■)] and PA phosphatidylcholine vesicles [30 mM (□)] were prepared for NMR spectroscopy as described under Materials and Methods and were irradiated at 3.2 ppm for selected intervals (50 ms to 5 s). The rate of integrated resonance intensity buildup was quantified by comparisons with steady-state NOE (5 s). All data points are the $\bar{X} \pm$ SE of at least three independent preparations.

deuterated dipalmitoylphosphatidylcholine, these results demonstrate that the observed interactions reflect intramolecular through-space dipolar coupling and do not result from interactions with other molecules of plasmenylcholine.

To compare and contrast the spatial relationship between the polar head group and the glycerol backbone in plasmenylcholine and phosphatidylcholine, additional TDNOE experiments were performed. Irradiation of the N–CH_3 resonance demonstrated that the initial buildup rate of resonance intensity for the methylene protons in the glycerol backbone was more rapid in phosphatidylcholine vesicles than in plasmenylcholine vesicles (Figure 4). If the modes of molecular motion in the polar head-group region are similar, then these results demonstrate that the average distance between the methylene protons of the glycerol backbone and the N–CH_3 protons is greater in plasmenylcholine than in phosphatidylcholine. Since prior X-ray diffraction, neutron diffraction, and NMR experiments have demonstrated a significant tilt of the polar head group in phosphatidylcholine (Pearson & Pascher, 1979; Buldt et al., 1978; Seelig et al., 1977), the present results indicate that the phosphocholine moiety in plasmenylcholine is in a more upright position than that in phosphatidylcholine.

Several unique features of the conformation of hydrated plasmenylcholine vesicles in the liquid-crystal phase may be deduced from these studies. First, the vinyl ether linkage is oriented with its protons no more than 90° from the plane formed by the two aliphatic chains. Second, the β-vinyl ether proton is equidistant (~3 Å) to both the α- and β-methylene protons of the *sn*-2 acyl chain, yet the α-vinyl ether proton is at least 5 Å from both the α- and β-methylene protons. Third, the phosphocholine moiety is more parallel to the membrane director in plasmenylcholine compared to phosphatidylcholine. Although phosphatidylcholine does not adopt a minimal energy conformation of its potential rotameric states (Schindler & Seelig, 1975), the distance constraints identified herein are entirely compatible with a low energy conformation of the proximal portion of the *sn*-2 acyl chain (trans–trans–trans). Taken together, these results suggest that the predominant time-averaged, but not the only, conformation of plasmenylcholine is similar to that shown in Figure 5. Although minor deviations from the proposed structure are not incompatible with the experimental data, the following conclusions seem inescapable: (1) the proximal portions of the *sn*-1 and *sn*-2 aliphatic chains in each plasmenylcholine molecule are in close

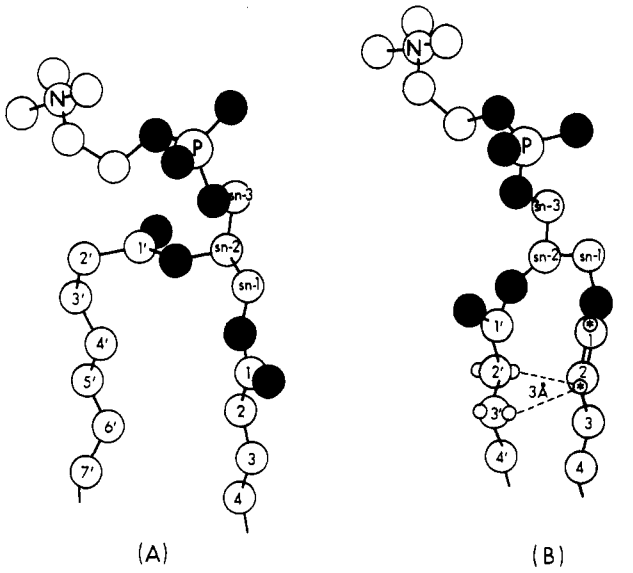

FIGURE 5: Comparison of the structure of phosphatidylcholine and the predicted structure of plasmenylcholine near the hydrophobic–hydrophilic interface. (A) The conformation of phosphatidylcholine has been redrawn from the coordinates previously obtained from X-ray diffraction studies of dimyristoylphosphatidylcholine (Pearson & Pascher, 1979). Support for this conformation of the phosphatidylcholine bilayer has been obtained by ^2H NMR. (B) This conformation of plasmenylcholine is proposed on the basis of the distances of the α- and β-vinyl ether protons in the *sn*-1 aliphatic chain to the α- and β-methylene protons in the *sn*-2 aliphatic chain deduced in this study. Essential features of this model include the following: (1) the proximal portions of the *sn*-1 and *sn*-2 aliphatic chains in plasmenylcholine are much closer than those in phosphatidylcholine; (2) the carbon atoms that comprise the proximal portion of the aliphatic chains in plasmenylcholine are in register (see text); (3) the plane formed by the oxygen atoms in the *sn*-1 and *sn*-2 chains of plasmenylcholine has a spatial relationship to the polar head group and the aliphatic chains which differs dramatically from that present in phosphatidylcholine. P and N refer to phosphorus and nitrogen atoms, respectively; the solid circles represent oxygen atoms; *sn*-1, -2, and -3 are carbon atoms in positions 1–3 of at the glycerol backbone, respectively; 1–4 and 1′–6′ refer to sequential carbon atoms in the *sn*-1 and *sn*-2 aliphatic chains, respectively; (*) represents the α- and β-vinyl ether protons that were irradiated during the TDNOE experiments.

spatial proximity; (2) the carbon atoms that comprise the proximal portion of the aliphatic chains in plasmenylcholine are in register (i.e., the first, second, third, etc. atoms in each chain are directly adjacent to their respective counterpart in the neighboring chain); (3) the plane formed by the oxygen atoms in the *sn*-1 and *sn*-2 chains of plasmenylcholine has a spatial relationship to the polar head group and aliphatic chains which differs dramatically from that present in phosphatidylcholine. Taken together, these results demonstrate that modest covalent alterations in the proximal portion of the *sn*-1 chain have dramatic effects on the spatial relationships and physical interactions present at the hydrophobic–hydrophilic interface in choline glycerophospholipids.

It is instructive to compare these results on the molecular conformation of plasmenylcholine to other studies examining differences in the biophysical characteristics of plasmenylcholine and phosphatidylcholine dispersions. First, although plasmenylcholine and phosphatidylcholine vesicles possess nearly identical internal volumes (Hermetter et al., 1985), the cross-sectional area of phosphatidylcholine monolayers is significantly larger than that of plasmenylcholine as assessed from the measurement of their surface pressure–molecular area isotherms (Smaby et al., 1983). Direct comparisons of the quadrapolar splitting of plasmenylcholine and phosphatidylcholine vesicles specifically deuterated at the C-2 carbon of

the *sn*-2 acyl chain demonstrated substantial differences in the splitting in one of the two diastereotopic deuterons (Pak et al., 1987). Similarly, Malthaner et al. (1987) have demonstrated differences in the quadrapolar splitting of plasmenylethanolamine/phosphatidylcholine binary mixtures (^2H present in the C-2 carbon of the *sn*-2 acyl chain of plasmenylethanolamine) compared to that in phosphatidylethanolamine dispersions. Since differences in the quadrapolar splitting between each diastereotopic deuteron are much smaller in plasmenylcholine than in phosphatidylcholine (Pak et al., 1987), these ^2H NMR studies on choline glycerophospholipid dispersions suggested that the proximal portion of the *sn*-2 chain in plasmenylcholine is more parallel to the membrane director than that in phosphatidylcholine (i.e., a larger degree of magnetic equivalence between the two diastereotopic deuterons is present). Thus, the proposed conformation of plasmenylcholine determined from the results of this study is compatible with a multiplicity of experimental evidence utilizing independent techniques.

Plasmalogens are highly enriched in arachidonic acid (Mueller et al., 1983; Gross, 1984, 1985; Ford & Gross, 1989a), and several phospholipases selectively hydrolyze plasmalogen substrate (Wolf & Gross, 1985b; Loeb & Gross, 1986; Angle et al., 1988). We speculate that the marked differences in the geometry of the polar atoms at the *sn*-1 and *sn*-2 positions in plasmenylcholine and phosphatidylcholine (including the molecular geometry and interactions of the *sn*-2 carbonyl) in conjunction with consequent alterations in their hydration state may contribute to the differential propensity of H_2O to act as a nucleophilic acceptor for each phospholipid subclass during phospholipolysis. Whatever the case, it seems likely that the profound differences in the molecular geometry of plasmenylcholine and phosphatidylcholine may underlie the biologic significance of ether-linked phospholipids in specific membrane compartments.

Acknowledgments

We gratefully appreciate the critical reading of the manuscript by Drs. Jacob Schaefer and Samuel Weissman.

References

Angle, M. J., Paltauf, F., & Johnston, J. M. (1988) *Biochim. Biophys. Acta 962*, 234–240.

Buldt, G., Gally, H. U., Seelig, A., Seelig, J., & Zaccai, G. (1978) *Nature 271*, 182–184.

Chilton, F. H., & Murphy, R. C. (1986) *J. Biol. Chem. 261*, 7771–7777.

Clore, G. M., & Gronenborn, A. M. (1985) *J. Magn. Reson. 61*, 158–164.

Ellena, J. F., Hutton, W. C., & Catiso, D. S. (1985) *J. Am. Chem. Soc. 107*, 1530–1537.

Feulgen, R., & Voit, K. (1924) *Pflugers Arch. Gesamte Physiol. Menschen Tiere 206*, 389–410.

Ford, D. A., & Gross, R. W. (1989a) *Proc. Natl. Acad. Sci. U.S.A. 86*, 3479–3483.

Ford, D. A., & Gross, R. W. (1989b) *Circ. Res. 64*, 173–177.

Gross, R. W. (1984) *Biochemistry 23*, 158–165.

Gross, R. W. (1985) *Biochemistry 24*, 1662–1668.

Hermetter, A., Lohner, K., Degovics, G., Laggner, P., & Paltauf, F. (1985) *Chem. Phys. Lipids 38*, 353–364.

Kuroda, Y., & Kitamura, K. (1984) *J. Am. Chem. Soc. 106*, 1–6.

Loeb, L. A., & Gross, R. W. (1986) *J. Biol. Chem. 261*, 10467–10470.

Malthaner, M., Hermetter, A., Paltauf, F., & Seelig, J. (1987) *Biochim. Biophys. Acta 900*, 191–197.

Mueller, H. W., Purdon, A. D., Smith, J. B., & Wykle, R. L. (1983) *Lipids 18*, 814–819.

Noggle, J. H., & Schirmer, R. W. (1971) *The Nuclear Overhauser Effect*, Academic Press, New York.

Pak, J. H., Bork, V. P., Norberg, R. E., Creer, M. H., Wolf, R. A., & Gross, R. W. (1987) *Biochemistry 26*, 4824–4830.

Pearson, R. H., & Pascher, I. (1979) *Nature 281*, 499–501.

Schindler, H., & Seelig, J. (1975) *Biochemistry 14*, 2283–2287.

Seelig, J., & Browning, J. L. (1978) *FEBS Lett. 92*, 41–44.

Seelig, J., Gally, H. U., & Wohlgemuth, R. (1977) *Biochim. Biophys. Acta 467*, 109–119.

Smaby, J. M., Hermetter, A., Schmid, P. C., Paltauf, F., & Brockman, H. L. (1983) *Biochemistry 22*, 5808–5813.

Wagner, G., & Wüthrich, K. (1979) *J. Magn. Reson. 33*, 675–680.

Wolf, R. A., & Gross, R. W. (1985a) *J. Lipid Res. 26*, 629–633.

Wolf, R. A., & Gross, R. W. (1985b) *J. Biol. Chem. 260*, 7295–7303.